

## Research article

# Effects of Ag-doped Content on Antimicrobial Activity and Substrate Color of Chromium Thin Films Deposited by DC Magnetron Sputtering

Pawarun Thanasriswad<sup>1\*</sup>, Rachsak Sakdanuphab<sup>1,4</sup>, Aparporn Sakulalavek<sup>4,5</sup> and Worakrit Woranantakij<sup>2,3</sup>

<sup>1</sup>College of Advanced Manufacturing Innovation, King Mongkut's Institute of Technology Ladkrabang Bangkok, Thailand

<sup>2</sup>Department of Biology, School of Science, King Mongkut's Institute of Technology Ladkrabang, Bangkok, Thailand

<sup>3</sup>Bioenergy Research Unit, School of Science, King Mongkut's Institute of Technology Ladkrabang, Bangkok, Thailand

<sup>4</sup>Department of Physics, School of Science, King Mongkut's Institute of Technology Ladkrabang, Bangkok, Thailand

<sup>5</sup>Electronic and Optoelectronic Device Research Unit, School of Science, King Mongkut's Institute of Technology Ladkrabang, Bangkok, Thailand

Curr. Appl. Sci. Technol. 2024, Vol. 24 (No. 1), e0255965; <https://doi.org/10.55003/cast.2023.255965>

Received: 15 September 2022, Revised: 10 November 2022, Accepted: 25 April 2023, Published: 1 June 2023

## Abstract

### Keywords

sputtering PVD;  
antibacterial agent;  
silver;  
mosaic target;  
ROS;  
gram-negative;  
gram-positive;  
CIE-L\*ab

Silver ions (Ag<sup>+</sup>) show promise as excellent antimicrobial agents to inhibit microbial growth on high-touch surfaces. In this study, Ag-doped Cr films were deposited using a DC magnetron sputtering system from a mosaic target. The Cr-Ag mosaic target was a 0.125-inch-thick Cr base (99.95% pure) with different diameters of Ag circle sheets mounted on the Cr target. The sputtering condition was kept at a DC power of 100W, working pressure of  $8.3 \times 10^{-3}$  mbar with Ar as the sputtering gas, and sputtering times of 15 and 30 min. The antimicrobial activity and efficiency were determined by standard testing (JIS Z 2801: 2000). The antibacterial performance was calculated from the antibacterial inhibition of the Ag-doped Cr films in bacterial solution (*Staphylococcus aureus* and *Escherichia coli*) after 24 h. The results showed that the Ag content was between 0.27 at% and 6.11 at% depending on the diameter of Ag and the deposition time. The minimum Ag content of 4.05 at% had an inhibition efficiency of 99.98% (*E. coli*) and 96.33% (*S. aureus*). The contact angle testing of Ag-doped Cr films showed hydrophobic behavior with the angle greater than 90 degrees. The optical color of the Ag-doped films was characterized by UV-vis spectroscopy (CIE testing). The film colors were significantly changed by the addition of Ag into the Cr films. The total color difference ( $\Delta E$ ) increased by 3-10 units compared to the reference chromium film and the Ag doping mainly affected +L\* (Lightness).

\*Corresponding author: Tel.: (+66)934598942

E-mail: 62609006@kmitl.ac.th

## 1. Introduction

According to the World Health Organization, illness caused by pathogenic bacteria is the second biggest incidence of death in children under the age of five [1]. Bacterial diseases have a significant impact on public health, due to the spreading of microbes facilitated by high-touch surfaces. Numerous people become infected after encountering contaminated surfaces such as doorknobs, handles, sink taps, etc. The ability of microorganisms to persist on surfaces is one factor that is particularly important in the spread of infectious diseases. Antimicrobial coatings have helped to reduce the number of bacteria spread on surfaces that are contacted by humans. Many scientists are currently interested in antibacterial films that are harmless to people and effective at inhibiting bacterial growth [2].

The magnetron sputtering technique is one of the most effective methods to fabricate high quality films for large scale production. This technique has been applied in many industries including the aircraft, chemical, and consumer product industries. It has been used in tooling and molds, optics, and has found use in medical applications [3-6]. In addition, sputtering is an excellent coating for corrosion resistance, wear resistance, and hardness. In this technique, the vacuum chamber of the sputtering system is evacuated, and argon gas (Ar) is introduced with applied DC high voltage. Ar plasma-ions are generated, and they bombard the target as atomic particles, causing the target to sputtered atoms which are deposited on the substrate. This process can produce a single layer or multilayer coating using single or multiple targets, respectively.

Silver (Ag) is known as an antibacterial agent element, and there is growing interest in its use as silver antimicrobial coatings in a variety of medical applications. Additionally, Ag has antibacterial properties against both gram-positive and gram-negative bacteria by releasing  $\text{Ag}^+$  ion into bacteria. When  $\text{Ag}^+$  ions interact with bacterial cells (peptidoglycan layer and cytoplasmic membrane) and accumulate in the cell, they inhibit cell division and growth by damaging the respiratory system, protein synthesis, and ribosomes. The ions damage and destroy DNA.  $\text{Ag}^+$  ions trigger bacterial cells to generate reactive oxygen species (ROS). As a result, the  $\text{Ag}^+$  ions expedite the generation of hydrogen peroxide, which causes the cytotoxic effect on bacterial cells [7-10]. Ag-ions can be released from bulk material or thin film under ambient conditions activated by oxygen and water.

Silver can be added to materials to improve their antibacterial properties, i.e., amorphous carbon (a-C), copper (Cu) and silicon (Si) [11-13]. Chromium (Cr) films have been used in various applications, including sanitary surfaces such as tabs, door locks, or bathroom fittings, but have no potential for antibacterial activity [14]. Improvement of antibacterial Cr films by Ag addition is facilitating new developments in the hygienic surface field.

In this work, the antibacterial performance, color differences from Cr film, and surface wettability of different Ag-doped Cr films were studied. The Ag content was minimized to achieve antibacterial inhibition efficiency and color tolerance. We employed a Ag-Cr mosaic target made of Ag metal placed into a Cr metallic matrix in this experiment. This method involved the use of a magnetron for sputtering multicomponent films. To gain higher material content in thin film, the content can be altered by changing the metal diameter.

## 2. Materials and Methods

### 2.1 Substrate preparation and thin film deposition

Brass sanitary grade substrates were used in the deposition of Cr and Ag-doped Cr films. The substrate dimensions were  $50 \times 50 \text{ mm}^2$  with a thickness of 3 mm. They were first cleaned with

acetone in an ultrasonic bath for 15 min to remove lipid, oxides, and other contaminants on the substrate surface. After the cleaning process, Cr and Ag-doped Cr films were deposited with a DC magnetron sputtering method using a mosaic target. A chromium-silver (Ag-Cr) mosaic target was used as a single target for combined metallic elements by varying the Ag diameter at the center of Cr target, as seen in Figure 1. The schematic of the mosaic target (Figure 1a) shows the Cr base target (purity of 99.95%) and Ag circle sheet (purity 99.95%) mounted at its center with double-sided conductive adhesive (carbon tape). In the theory, collisions are considered to occur as described in the hard-sphere model. The sputtering of the target with energetic ions or recoil atoms results from cascades of atomic collisions [15-17]. The sputter yield is expressed by the relationship between the incident energy and the number of atoms ejected/sputtered from target material to substrate. To control the small amount of Ag, the center of the target has a lower magnetic field, which decreases collisions with scattered particles from the target [18]. Figure 2 shows that substrates were placed at 60 mm away from the target and the substrate rotation speed was 8 rpm to improve the uniformity of the thin films. A pre-sputtering process was employed before deposition to remove contamination from the surface to ensure good adhesion between surface and film coating. Table 1 shows the sputtering conditions used in the deposition of Cr and Ag-doped Cr films. Various diameters of Ag ranged from 6 mm to 13 mm, and sputtering time of 15 and 30 min were investigated. Ag content in Cr films influences antibacterial efficiency, surface wettability, and color tolerance.

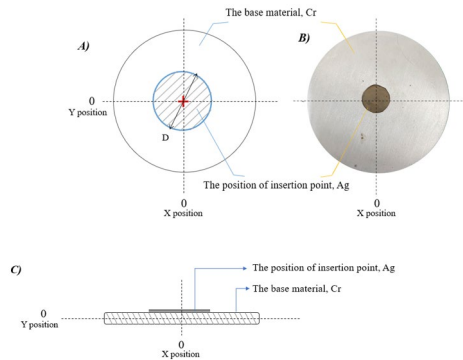


**Figure 1.** a) Schematic of the mosaic Cr-Ag sputtering target, b) Mosaic target pattern, c) Schematic of the mosaic Cr-Ag sputtering target cross-section

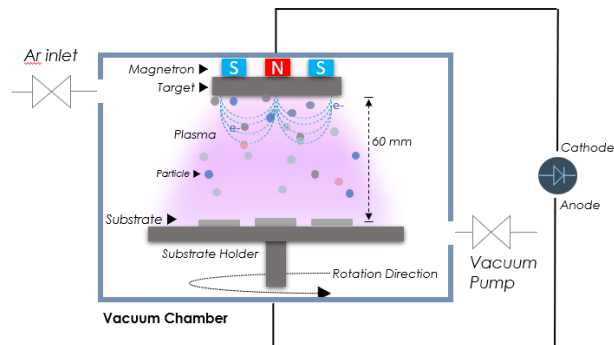


**Figure 2.** Schematic diagram of the PVD sputtering

**Table 1.** Deposition process conditions of Cr-thin film and Ag-doped Cr thin films

Conditions	Thin Film Material	
	Cr Thin Film	Ag-doped Cr Thin Films
Ag diameter (mm)	N/A	6, 8, 10, 13
Sputtering time (min)	15	15 and 30 min
Base pressure (mbar)	$6 \times 10^{-6}$	$6 \times 10^{-6}$
Sputtering pressure (mbar)	$8.3 \times 10^{-3}$	$8.3 \times 10^{-3}$
Sputtering power (W)	100	100
Ar flow rate (sccm)	30	30
Substrate rotation (rpm)	8	8

## 2.2 Chemical and physical characterization

The chemical composition of the Ag-doped Cr thin films was characterized using energy dispersive spectroscopy (EDS), and an Oxford Xmax silicon drift detector 20 mm<sup>2</sup> was used. The atomic composition of Ag depends on the diameter of Ag circle sheet and the deposition time. The wettability was measured on a Contact Angle System OCS, Data Physics Instruments, using the DI solution with volume 5 L and dosing rate 1 L/s in the capillary 205 μL to determine the hydrophobic and surface properties. Hydrophobic properties of the Ag-doped Cr films affected bacterial adhesion and bacterial growth [19]. The color measurement of the Ag-doped Cr thin films with different Ag content was measured using the Commission on Illumination (CIE) method. The absorption was recorded with a UV-VIS Spectrophotometer (Shimadzu, UV-2600i). The CIE testing utilizes the 3-axis (L\* a\* b\*) color space which is in the visible region of the spectrum. L\* is a measure of light to dark, a\* is a measure of hue magnitude (-a\* is green to +a\* is red color) and b\* is a measure of saturation magnitude (-b\* is blue to +b\* is yellow color). Delta-E is a measure of the difference of two colors expressed on a scale from 0 to 10. Medium difference, the ΔE in range 0-10, can be observed by untrained observer. Delta-E was calculated by equation (1) [20, 21]:

$$\Delta E_{ab}^* = \sqrt{(L_2^* - L_1^*)^2 + (a_2^* - a_1^*)^2 + (b_2^* - b_1^*)^2} \quad (1)$$

## 2.3 Antibacterial inhibition efficiency

The Cr and Ag-doped Cr thin films were characterized by antibacterial survival test for both gram-negative and gram-positive bacteria, using JIS Z 2801. This standard test measures the antibacterial efficiency on surfaces such as plastic, textile, wood, metal, etc. Bacterial species used for testing in this study were gram-negative *Escherichia coli* ATCC 25922 and gram-positive *Staphylococcus aureus* ATCC 25923 cultured in trypticase soy broth (TSB). From bacterial suspension ( $1.5 \times 10^6$  CFU/mL), 10 μL was dropped on the top of the coated and uncoated (control) samples. A sterile plastic film (4 cm<sup>2</sup>) was placed on top as a cover, and the samples were then incubated at 37°C for 24 h. After incubation, recovery was performed by dropping 10 μL of TSB on the materials, and a tenfold serial dilution was performed to enable colony count.

Then, the solution was spread onto tryptic soy agar (TSA) plates and incubated at 37°C for 24 h as shown in Figure 3a and Figure 3c (samples before treatment). Figure 3b and Figure 3d show the samples after treatment with *S. aureus* and *E. coli* after 24 h incubation. All measurements were repeated three times with a control sample. After that, the visible colonies on the TSA plates were counted [22-25], and the percentages of bacterial inhibition ( $R$ ),  $R$  were calculated according to equation (2):

$$R = (A - B) / A \quad (2)$$

where  $R$  is the percentage of bacterial inhibition,  $A$  is the number of visible bacterial colonies on the control test plate (CFU/mL) after 24 h, and  $B$  is the number of visible bacterial colonies on the treated test plate (CFU/mL) after 24 h.

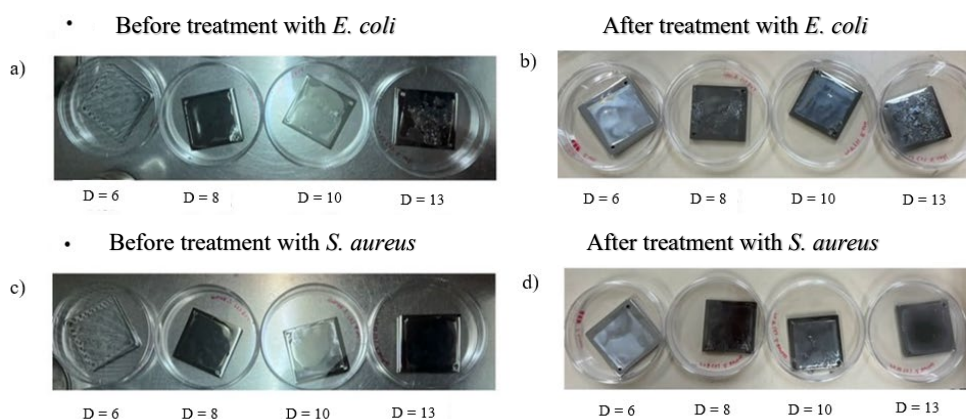


**Figure 3.** Testing of Ag-doped Cr thin films with different Ag content

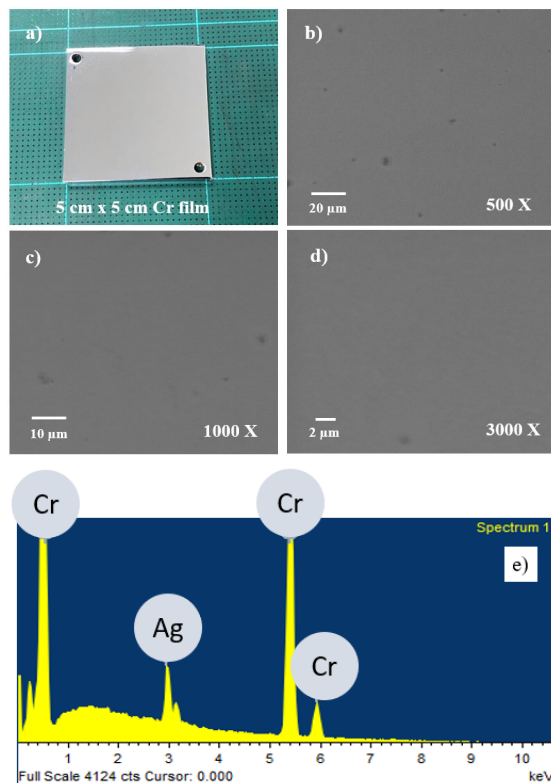
### 3. Results and Discussion

#### 3.1 Chemical composition of thin films

The effect of Ag diameter and deposition time on the chemical concentration of Ag-doped Cr films are shown in Table 2. The atomic concentration of Ag in the film increases with the diameter of Ag on the Cr target, and the film thickness and at% Ag also linearly increase with deposition time [26, 27]. The minimum % of Ag deposited was 0.27 at%, and this is for a Ag diameter of 6 mm and deposition time of 15 min, while the maximum deposited Ag content was 6.11 at%, which was for Ag diameter of 13 mm and deposition time of 30 min. Figure 4 show the surfaces and EDS spectra of Ag-doped Cr films with the maximum Ag content. The smooth surface and homogeneity of the thin films can be seen in Figure 4(a). These results show that we succeeded in producing Ag-doped Cr thin film and controlled the Ag content in the film by using the mosaic target approach. The Ag content is mainly important for the efficiency of antibacterial inhibition, which will be described in Section 3.4.

**Table 2.** Chemical composition of Ag-doped Cr thin film with different Ag diameter of Cr target and deposition time

Deposition Time (min)	Ag Diameter of Mosaic Target (mm)	Ag (at%)	Cr (at%)
<b>Cr Thin Film</b>	Cr target (Purity 99.95%)	N/A	N/A
<b>15 min</b>	6	0.27	99.73
	8	0.68	99.32
	10	0.94	99.06
	13	1.52	98.48
<b>30 min</b>	6	1.71	98.29
	8	2.91	97.09
	10	4.05	95.95
	13	6.11	93.89

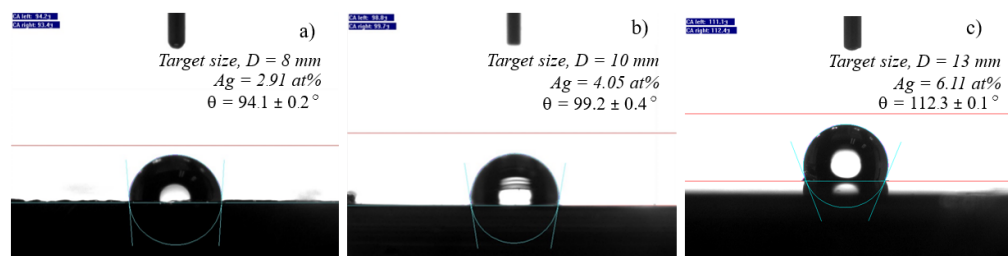
**Figure 4.** The results of Ag-doped Cr thin film deposited by Ag ( $\theta = 13$  mm) and deposition time of 30 min: (a) photo image, (b), (c) and (d) SEM images at 500X, 1000X, and 3000X, respectively, and (e) EDS spectra

### 3.2 Surface wettability of thin films

A key factor in antibacterial enhancement is surface wettability. Hydrophobicity and low surface energy result in significant antibacterial inhibition because the high surface energy can increase the adhesion performance of bacteria on their surface. Table 3 shows the contact angle of Ag-doped Cr films with different deposition conditions. The reference Cr thin film had lowest contact angle, which was  $47.3^\circ$ . However, when Ag was introduced into Cr film, the contact angle was increased to  $66^\circ$  in the case of the samples produced with Ag diameter of 8 mm and deposition time of 15 min. Furthermore, the contact angle increased to  $112.4^\circ$  for film with Ag diameter of 13 mm and deposition time of 30 min, as shown in Table 3. The results indicate that the contact angle continuously increased with Ag content increase. Figure 5 (a-c) shows stereo microscope images of water contact angles of Ag-doped Cr films deposited using Ag diameters of 8, 10, and 13 mm, and the contact angles are  $94.1^\circ$ ,  $99.2^\circ$  and  $112.3^\circ$ , respectively. Domínguez-Meister *et al.* [11] showed that amorphous carbon doped Ag film had a contact angle above  $110^\circ$  and was independent of Ag content when compared with  $85^\circ$  without doped silver in amorphous carbon film. Their result also showed that the adhesion of bacteria in low surface energy was decreased. Baba *et al.* [19] studied the variation of water contact angle with Ag content change. They found that the angle increased with Ag content, starting from  $65.6^\circ$  for Ag 3.8 at% and increasing to  $93.3^\circ$  for 27 at%, with some variation. Our results agree with the findings of Domínguez-Meister *et al.* and Baba *et al.* [11, 19].

**Table 3.** Relationship between water contact angle and Ag content of Ag-doped Cr thin films with different Ag diameter and deposition time

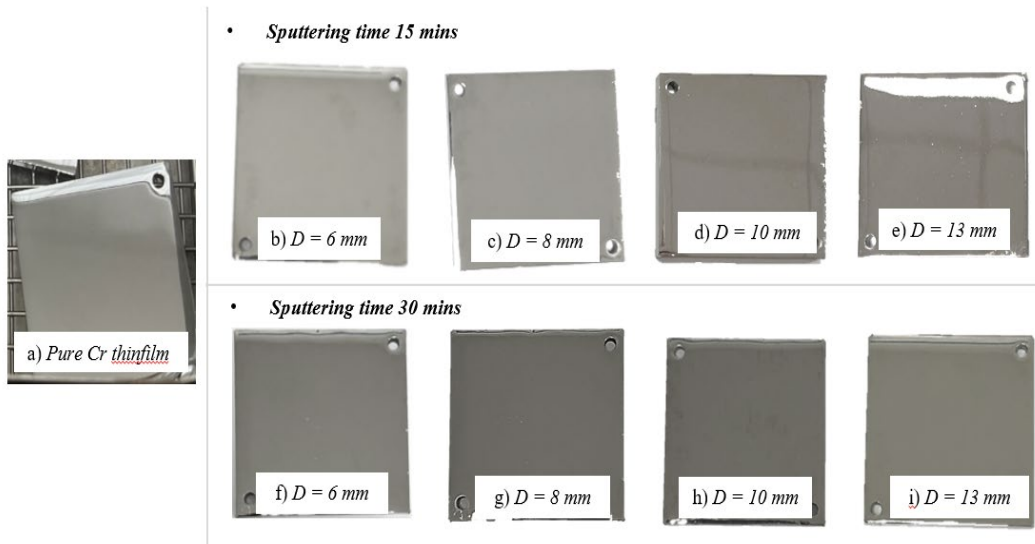
Deposition Time (min)	Ag Sizing (mm)	Ag Content (at%)	Contact Angle ( $\theta$ )
Cr thin film	0	0	$47.3 \pm 0.3$
15 min	6	0.27	$64.5 \pm 0.4$
	8	0.68	$66.1 \pm 0.2$
	10	0.94	$67.2 \pm 0.1$
	13	1.52	$79.9 \pm 0.2$
30 min	6	1.71	$83.3 \pm 0.3$
	8	2.91	$94.1 \pm 0.2$
	10	4.05	$99.2 \pm 0.4$
	13	6.11	$112.3 \pm 0.1$



**Figure 5.** The contact angle of the Ag-doped Cr thin films deposited at 30 min with different Ag diameter: a) D = 8 mm, b) D = 10 mm, and c) D = 13 mm

### 3.3 Color determination

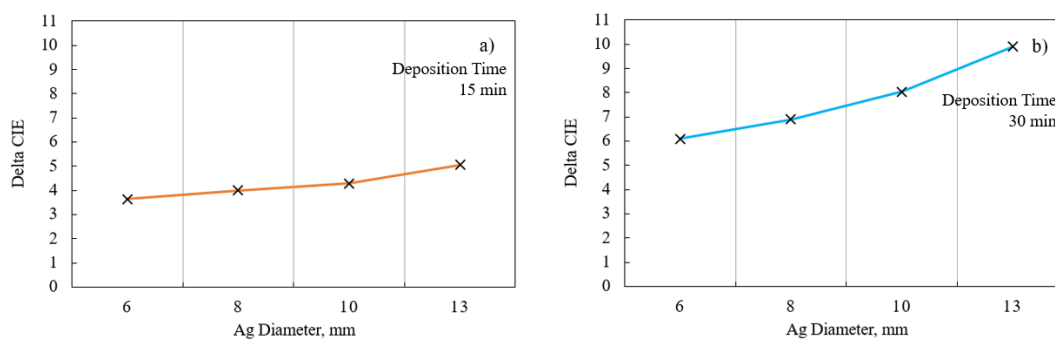
Figure 6 shows images of the Ag-doped Cr thin films with different deposition conditions of Ag diameter and deposition time. The color of Ag-doped Cr films became darker compared with the reference Cr film (Figure 6a) when the Ag content increased, as seen in Figures 6b-6i. The film deposited using Ag diameter of 6 mm at 15 min (Figure 6a) had the lowest color difference while the film deposited using Ag diameter of 13 mm at 30 min (Figure 6h) had the highest color difference due to the highest Ag content. The quantitative color of the Ag-doped Cr films was observed by CIE-L\*ab measurement and was compared with reference Cr film, as shown in Table 4. The brightness of the Ag-doped Cr films ( $L^*$ ) decreased from 80.43 to 71.46 as Ag content increased, and this was related to the dark color in Figure 5 and related to the increasing thickness with deposition time [28]. The brightness ( $L^*$ ) of coatings corresponds to the Ag content in Cr films. This is due to the silver atoms chemically reacting with the environment and causing silver to turn black (formation of silver oxide and silver sulfide). The brightness of the coating decreases with silver concentration. However, the  $a^*$  and  $b^*$  values of Ag-doped Cr films increased with increase in Ag content. According to the references of CIE-L\*ab of Cr ( $L^* = 80.43$ ,  $a^* = -0.95$ ,  $b^* = -1.85$ ), the color difference of Ag-doped Cr films could be determined by delta CIE-L\*ab ( $\Delta E$ ), as shown in Figure 7. The colorimetric test results were related to the Ag content, which varied with the deposition conditions. We were able to classify the  $\Delta E$  values into two regions based on the perception of human eye, which has a threshold of  $\Delta E < 5$ . The films with Ag content between 0.27-0.94 at% had  $\Delta E$  in the range of  $3 < \Delta E < 5$ , whereas the films with Ag content between 1.52-6.11 at% had  $\Delta E$  of  $5 \leq \Delta E < 10$ .



**Figure 6.** Images of reference Cr film (a) and Ag-doped Cr films with different Ag diameter and deposition time (b)-(i)

**Table 4.** Relationship between CIE-L\*ab result and Ag content of Ag-doped Cr films with different Ag diameter and deposition time

Deposition Time (min)	Ag Sizing (mm)	Ag Content (at%)	L*	a*	b*
Cr thin film	0	0	80.43	-0.95	-1.85
15 min	6	0.27	79.24	-0.45	1.55
	8	0.68	78.81	-0.06	1.69
	10	0.94	78.44	0.03	1.82
	13	1.52	77.61	0.09	2.2
30 min	6	1.71	76.13	0.11	2.34
	8	2.91	75.23	0.11	2.55
	10	4.05	74.02	0.21	2.85
	13	6.11	71.46	0.27	2.14

**Figure 7.** Delta CIE of Ag-doped Cr films of different Ag diameters at deposition times of (a) 15 min and (b) 30 min

### 3.4 Antibacterial efficiency of thin films

Ag-doped Cr films were tested for antibacterial inhibition against *E. coli* and *S. aureus*. After 24 h, the visible colony was counted, and the results are shown in Table 5. The reference Cr film was observed with the colony count of  $1.8 \times 10^9$  CFU/mL. The Ag-doped Cr films with Ag content of 1.71 at% and 2.91 at% had the colony count of  $1.93 \times 10^9$  CFU/mL and  $1.52 \times 10^9$  CFU/mL for *E. coli* and the colony count of  $1.95 \times 10^9$  CFU/mL and  $1.1 \times 10^9$  CFU/mL for *S. aureus*, respectively. For the percentage of bacterial inhibition, it was found that the film that contained less than 2.91% had a weak ability and only inhibited bacterial growth by 16.02% for *E. coli* and 9.09% for *S. aureus*. However, when Ag content was increased to 4.05 at%, it was observed that the colony count had decreased to  $7.1 \times 10^5$  CFU/mL for *E. coli* and  $4.4 \times 10^7$  CFU/mL for *S. aureus*. Thus, the results of percentage inhibition showed that the Ag at 4.05 at% or over had a strong ability to inhibit bacterial growth with a reduction of 99.98% for *E. coli* and 96.33% for *S. aureus* for Ag at 4.05 at%.

**Table 5.** Relationship between deposition conditions and the antibacterial efficiency

Deposition Time (min)	Ag Sizing (mm)	Ag Content (at%)	Gram-negative		Gram-positive	
			<i>(E. coli)</i>		<i>(S. aureus)</i>	
			Colony	Inhibition (%)	Colony	Inhibition (%)
Cr thin film	0	0	$1.81 \times 10^9$	N/A	$1.21 \times 10^9$	N/A
Ag-doped Cr thin film	6	1.71	$1.93 \times 10^9$	N/A	$1.95 \times 10^9$	N/A
30 min	8	2.91	$1.52 \times 10^9$	16.02%	$1.1 \times 10^9$	9.09%
	10	4.05	$7.1 \times 10^5$	99.61%	$4.44 \times 10^7$	96.33%
	13	6.11	$3.41 \times 10^5$	99.98%	$2.88 \times 10^7$	97.62%

According to Ishida [8], Xiu, *et al.* [9] and Ouay and Stellacci [10], the effects of Ag<sup>+</sup> ions against *S. aureus* peptidoglycan cell wall are due to inhibition of peptidoglycan elongation caused by regulation of peptidoglycan synthetic transglycosylase and transpeptidase, and enhancement of the activation of peptidoglycan autolysins of amidases. On the contrary, the antibacterial effects on *E. coli* cell wall are caused by the destruction of outer membrane structure of bacterial cells by degradative enzymes of lipoproteins at N- and C-terminals, and by the inhibition of peptidoglycan elongation. Silver ions induced ROS generations such as O<sub>2</sub><sup>-</sup>, H<sub>2</sub>O<sub>2</sub>, + OH, OH producing in bacterial cell wall occur and lead to oxidative stress. DNA damage may be due to Ag<sup>+</sup>-coordinated complex formations by Ag<sup>+</sup> substitution within hydrogen bonds in DNA base pairs. Antibacterial activity of silver nanoparticles is primarily due to the influence of Ag<sup>+</sup> release. In addition, antibacterial activity could be controlled, and environmental impacts could also be mitigated by modulating Ag<sup>+</sup> release, probably through manipulation of oxygen availability, particle size, shape, and/or type of coating [8-10]. Jung *et al.* [29] showed that silver ion of spinning bucket in washing machine could effectively inhibit both gram-positive and gram-negative bacteria by the release of the ions to eliminate bacteria from fabrics in the washing machine. Hsieh *et al.* [30] showed that Ag content of 5 at% doped on TaON had 47% antibacterial efficiency after 24 h without light irradiation. Our results showed that the film with the Ag content at 4.05 at% or over effectively inhibited *E. coli* and *S. aureus*. Therefore, this type of film properties could be used as antibacterial material.

#### 4. Conclusions

In conclusion, Ag-doped Cr films were deposited by DC magnetron sputtering using Ag-Cr mosaic target. The Ag contents deposited varied from 0.27 to 6.11 at%, and these values were obtained by using 6 mm Ag diameter and 15 min deposition time, and 13 mm Ag diameter and 30 min deposition time, respectively. The increase of Ag contents in Cr films was related to the increase of contact angles and the inhibition of bacteria. A hydrophobic surface was observed for film with Ag content more than 2.9 at% for Ag diameter of 8 mm at deposition time of 30 min. Ag-doped Cr film with Ag content of 4.05 at% showed effective antibacterial activities of 99.98% inhibition for gram-negative *E. coli* and 96.33% for gram-positive *S. aureus*. In addition, the antibacterial activities were closely related with the silver content of the film. However, a color difference ( $\Delta E$ ) of greater than 5 was obtained when the Ag content was greater than 1 at%. The films became darker with the increase of Ag content. The color tolerance will be interested in further studies for sanitary applications.

## References

- [1] WHO, 2021. *Antibiotic Resistance*. [online] Available at: <https://www.who.int/news-room/fact-sheets/detail/antibiotic-resistance>.
- [2] WHO Africa, 2021. *Diarrhoeal Disease*. [online] Available at: <https://www.afro.who.int/health-topics/child-health#>.
- [3] Fox-Rabinovich, G., Paiva, J.M., Gershman, I., Aramesh, M., Cavelli, D., Yamamoto, K., Dosbaeva, G. and Veldhuis, S., 2016. Control of self-organized criticality through adaptive behavior of nano-structured thin film coatings. *Entropy*, 18(8), <https://doi.org/10.3390/e18080290>.
- [4] Hoche, H., Groß, S. and Oechsner, M., 2014. Development of new PVD coatings for magnesium alloys with improved corrosion properties. *Surface and Coatings Technology*, 259, 102-108, <https://doi.org/10.1016/j.surfcoat.2014.04.038>.
- [5] Korhonen, H., Syväluoto, A., Leskinen, J.T.T. and Lappalainen, R., 2018. Optically transparent and durable Al<sub>2</sub>O<sub>3</sub> coatings for harsh environments by ultra short pulsed laser deposition. *Optics and Laser Technology*, 98, 373-384, <https://doi.org/10.1016/j.optlastec.2017.07.050>.
- [6] Baptista, A., Silva, F., Porteiro, J., Míguez, J. and Pinto, G.F., 2018. Sputtering physical vapour deposition (PVD) coatings: a critical review on process improvement and market trend demands. *Coatings*, 8(11), <https://doi.org/10.3390/coatings8110402>.
- [7] Oruma, U.S., Asegbeloyin, J.N., Eze, F.U. and Chah, K.F., 2014. Synthesis, screening of (2z, 4z)-4-(pyrimidin-2-ylimino) pent-2-en-2-ol (PIP) and its copper (ii) and chromium (iii) complexes. *International Journal of Chemical Sciences*, 12(1), 136-144.
- [8] Ishida T., 2018. Antibacterial mechanism of Ag<sup>+</sup> ions for bacteriolyses of bacterial cell walls via peptidoglycan autolysis and DNA damages. *MOJ Toxicology*, 4(5), 345-350, <https://doi.org/10.15406/mojt.2018.04.00125>.
- [9] Xiu, Z.-M., Zhang, Q.-B., Puppala, H.L., Colvin, V.L. and Alvarez, P.J.J., 2012. Negligible particle-specific antibacterial activity of silver nanoparticles. *Nano Letters*, 12, 4271-4275, <https://doi.org/10.1021/nl301934w>.
- [10] Ouay, B.L. and Stellacci, F., 2105. Antibacterial activity of silver nanoparticles: A surface science insight. *Nano Today*, 10(3), 339-354, <https://doi.org/10.1016/j.nantod.2015.04.002>.
- [11] Domínguez-Meister, S., Rojas, T.C., Frías, J.E. and Sánchez-López, J.C., 2019. Silver effect on the tribological and antibacterial properties of a-C: Ag coatings. *Tribology International*, 140, <https://doi.org/10.1016/j.triboint.2019.06.030>.
- [12] Valodkar, M., Modi, S., Pal, A. and Thakore, S., 2011. Synthesis and anti-bacterial activity of Cu, Ag and Cu–Ag alloy nanoparticles: A green approach. *Materials Research Bulletin*, 46(3), 384-389, <https://doi.org/10.1016/j.materresbull.2010.12.001>.
- [13] Liu, X., Lin, Y., Xiang, J., Hao, J. and Wan, X., 2018. Dual-doped (Si-Ag) graphite-like carbon coatings with ultra-low friction and high antibacterial activity prepared by magnetron sputtering deposition. *Diamond and Related Materials*, 86, 47-53, <https://doi.org/10.1016/j.diamond.2018.04.016>.
- [14] Raza, M.A., Kanwal, Z., Riaz, S. and Naseem, S., 2016. Antibacterial performance of chromium nanoparticles against *Escherichia coli*, and *Pseudomonas aeruginosa*. *The 2016 World Congress on Advances in Civil, Environmental and Materials Research (ACEM'16)*, Jeju Island, Korea, August 28-October 1, 2016, pp. 1-6.
- [15] Daniels, S., 1999. *PVD Process Modeling and Description into Sub-micron Features*. Ph.D. Dublin City University, Ireland.
- [16] Geiser, J. and Blankenburg, S., 2012. Monte Carlo simulations concerning elastic scattering with application to DC and high power pulsed magnetron sputtering for Ti<sub>3</sub>SiC<sub>2</sub>. *Communications in Computational Physics*, 11(5), 1618-1642, <https://doi.org/10.4208/cicp.210211.270511a>.

- [17] Mattox, D.M., 1998. *Handbook of Physical Vapor Deposition (PVD) Processing*. [online] Available at: <https://www.sciencedirect.com/book/9780815514220/handbook-of-physical-vapor-deposition-pvd-processing>.
- [18] Feist, C., Plankensteiner, A. and Winkle, J., 2013. Studying target erosion in Planar sputtering magnetrons using a discrete model for energetic electrons. *Proceedings of the 2013 COMSOL Conference*, Reutte, Austria, October 23-25, 2013, pp. 1-7.
- [19] Baba, K., Hatada, R., Flege, S., Ensinger, W., Shibata, Y., Nakashima, J., Sawase, T. and Morimura, T., 2013. Preparation and antibacterial properties of Ag-containing diamond-like carbon films prepared by a combination of magnetron sputtering and plasma source ion implantation. *Vacuum*, 89, 179-184, <https://doi.org/10.1016/j.vacuum.2012.04.015>.
- [20] Cui, J., Shao, Y., Zhang, H., Zhang, H. and Zhu, J., 2021. Development of a novel silver ions-nanosilver complementary composite as antimicrobial additive for powder coating. *chemical engineering journal*, 420, <https://doi.org/10.1016/j.cej.2020.127633>.
- [21] Chang, T., Sepati, M., Herting, G., Leygraf, C., Kuttuva Rajarao, G., Butina, K., Richter-Dahlfors, A., Blomberg, E. and Odnevall, W.I., 2021. A novel methodology to study antimicrobial properties of high-touch surfaces used for indoor hygiene applications-A study on Cu metal. *PLoS ONE*, 16(2), <https://doi.org/10.1371/journal.pone.0247081>.
- [22] Japanese Standard Association, 2000. *JIS Z 2801: 2010 Antibacterial Products – Test for Antibacterial Activity and Efficacy*. Tokyo: Japanese Standard Association.
- [23] Cristina-Ş.A., Cătălin V., Anca C.P., Adrian E.K., Iulian P., Alina V., Sarah C., Marius M., Radu M., Mihaela B. and Mihaela I., 2022. Synthesis and investigation of antibacterial activity of thin films based on TiO<sub>2</sub>-Ag and SiO<sub>2</sub>-Ag with potential applications in medical environment. *Nanomaterials*, 12(6), <https://doi.org/10.3390/nano12060902>.
- [24] Tan, G.L., Tang, D., Dastan, D., Jafari, A., Shi, Z., Chu, Q.Q., Silva, J.P.B. and Yin, X.T., 2021. Structures, morphological control, and antibacterial performance of tungsten oxide thin films. *Ceramics International*, 47(12), 17153-17160, <https://doi.org/10.1016/j.ceramint.2021.03.025>.
- [25] Hsieh, J.H., Tseng, C.C., Chang, Y.K., Chang, S.Y. and Wu, W., 2008. Antibacterial behavior of TaN-Ag nanocomposite thin films with and without annealing. *Surface and Coatings Technology*, 202(22-23), 5586-5589, <https://doi.org/10.1016/j.surfcoat.2008.06.107>.
- [26] Prathumsit, J., Gitgeatpong, G., Phae-ngam, W., Chananonnawathorn, C., Lertvanithphol, T. and Horprathum, M., 2020. The effect of thickness on the properties of Zr-Hf-N thin films prepared by reactive Co-magnetron sputtering. *Proceedings of the Second Materials Research Society of Thailand International Conference*, Pattaya, Thailand, July 10-12, 2019, pp. 120004-1-120004-5.
- [27] Baptista, A., Silva, F., Porteiro, J., Míguez, J. and Pinto, G., 2018. Sputtering physical vapour deposition (PVD) coatings: a critical review on process improvement and market trend demands. *Coatings*, 8(11), <https://doi.org/10.3390/coatings8110402>.
- [28] Zheng, B., Wong, L.P., Wu, L.Y.L. and Chen, Z., 2017. Identifying key factors towards highly reflective silver coatings. *Advances in Materials Science and Engineering*, 2017, <https://doi.org/10.1155/2017/7686983>.
- [29] Jung, W.K., Koo, H.C., Kim, K.W., Shin, S., Kim, S.H. and Park, Y.H., 2008. Antibacterial activity and mechanism of action of the silver ion in *Staphylococcus aureus* and *Escherichia coli*. *Applied and Environmental Microbiology*, 74(7), 2171-2178, <https://doi.org/10.1128/AEM.02001-07>.
- [30] Hsieh, J.H., Chang, C.C., Li, C., Liu, S.J. and Chang, Y.K., 2010. Effects of Ag contents on antibacterial behaviors of TaON-Ag nanocomposite thin films. *Surface and Coatings Technology*, 205, 5337-5340, <https://doi.org/10.1016/j.surfcoat.2010.08.010>.